Journal of Simulation and Analysis of Novel Technologies in Mechanical Engineering
15 (2) (2023) 0037~0051

Research article

Stress analysis of non-linearly variable thickness rotating disk in gas turbine engine using hyper-geometric method

Behrooz Shahriari[1,*], Nedasadat Seddighi[2]

[1]*Faculty of Mechanics, Malek Ashtar University of Technology, Isfahan, Iran*

[2]*Mechatronic Sanaat Sepahan Co., Isfahan, Iran*

[*]shahriari@mut-es.ac.ir

(Manuscript Received --- 27 Apr. 2023; Revised --- 28 June 2023; Accepted --- 03 July 2023)

Abstract

In this paper, the numerical and exact analytical calculation of elastic strains and stresses in gas turbine engine rotating disk with variable thickness, subjected to temperature gradient are presented. Galerkin method is applied to solve any kind of profiles with arbitrary thickness, temperature and density functions while the other numerical and analytical methods used in previous works, are applied to profiles with certain thickness functions. Therefore, a comprehensive approach that takes all the circumstances into account was used in an attempt to fill this gap. To verify the numerical method, a few examples of rotating disks with non-linear variable thicknesses were solved using the analytical method as a reference method and their results were compared with numerical solution. A good agreement between numerical and analytical solutions was observed. In the analytical part, a new method to convert equilibrium equation of rotating disks to hyper-geometric differential equation was provided and then it was solved. Using hyper-geometric method is the main novelty of this research. The distributions of radial displacement and stresses were obtained and an appropriate comparisons and discussions were made at the same environmental conditions.

Keywords: Gas turbine engine, Rotating disk, Non-linearly variable thickness and density, Stress analysis, Hyper-geometric method

1- Introduction

Rotating disks are of practical concern in many fields of engineering such as mechanical, marine and aerospace industries including gas turbine engines like turbojet, turbofan, turboprop, and turbo shaft engines; gears, turbo-machinery, flywheel systems turbo pumps, turbo generators and centrifugal compressors. The analysis of stress and strain distribution in variable thickness disks rotating at high speeds is important for a better understanding of the behavior and optimum design of rotors. For example, the stresses owing to centrifugal loads can have important effects on their strength and safety. Thus, optimization and

control of displacement and stress fields can help to reduce the overall weight and costs, especially in the aerospace industry. Stress analysis of variable thickness disks may be performed using the approach written by Timoshenko [1] with Grammel's method [2], or numerical method, such as the finite element or finite difference methods [3-5], numerical methods that use truncated Taylor's expansion [6], numerical integration [7], and boundary elements method [8].

Disk with uniform strength was designed by De Laval [9, 10]. The profile of this disk was portrayed by an exponential thickness function. A disk with a uniform strength profile must be solid, and at the outer edge, it has a rim where the blade roots are attached. Another variable-thickness profile was developed by Stodola [11], and it was introduced by a hyperbolic relationship given as a reference thickness multiplied by the variable raised to an exponent. The solid disk does not define by this profile but by constant thickness disks, annular disks; diverging disks, converging disks; which are featuring linear and non-linear thickness distribution. Converging conical disk was the third variable-thickness profile introduced by Honegger [12]. Giovannozzi [13] extended the Honegger's linear function, and developed its application to conical disks with diverging profile. Thickness function introduced by Honegger and Giovannozzi was further generalized by Güven [14] by extending a power of a linear function. The variation of which rests on the fourfold infinity of profiles, convex and concave, diverging and converging.

In the last decade, Rotating disk with constant density and variable thickness in power linear function form was studied [15, 16], in the framework of investigation which also focused on rotary velocity causing plastic deformation. Eraslan [17] investigated elastic and plastic deformation, for identical profile disks with non-isothermal conditions.

Recently, elastic stress analysis of rotating converging conical disks subjected to thermal load has been studied by Vivio and Vullo [18]. Semi-exact solution of elastic rotary disk by homotopy perturbation has been examined by Hojjati and Jafari [19]. Finite Difference Method for a rotating annular disk has been investigated by Zenkour and Mashat [20] without consideration of thermal conditions. Zenkour and Mashat considered a rotating annular disk with Runge-Kutta Method in another study [21]. Nejad et al. [22] derived a semianalytical solution for determination of displacements and stresses in a rotating cylindrical shell with variable thickness under uniform pressure, using disk form multilayers. Using Disk form multilayers, Mohammad Zamani Nejad et al., [23] elastic analysis of rotating thick truncated conical shells subjected to uniform pressure. Bagheri et al. [24] presented an analytical study of micro-rotating disks with angular acceleration on the basis of the strain gradient elasticity. Abdalla [25] presented a thermo-mechanical analysis and optimization of functionally graded rotating disks. Dinkar Sharma et al. [26] investigated thermo-elastic characteristics in functionally graded rotating disks using finite element method. These thermo-elastic characteristics of disk were plotted for various values of non-homogeneity parameter under power law distribution of material properties.

In the present study, the focus was on the numerical solution of the second-order differential equation defining the stress and

strain states of the isotropic rotary disk, that is symmetrical to the middle axis. Galerkin method is a subset of weighted residual techniques that reduces a continuous equilibrium problem to an approximately equivalent equilibrium problem with many degrees of freedom. It is a comprehensive general approach that all environmental conditions impose on the disks, boundary conditions, and also profiles of all types are included. Galerkin method also does not show the limitations of the approaches known up to now. The environmental conditions and boundary conditions can be pointed to thermal loads acting on disks and density variation and external loads applied to the inner and outer radius of the presence hub and rim, respectively. So, this method solves equilibrium equation of rotating disks for any arbitrary function of temperature, density and thickness. In the rest of work, an analytical method for parabolic rotating disks with variable density under the effect of the temperature gradient along the radius assuming the third order polynomial function for both of them is provided. Here, the equation of equilibrium by a linear combination of two independent hyper-geometric functions regardless of the point of singularity is resolved. Also, the proposed closed-form solution does not blind the physical meaning of its particular integral. To convert homogeneous part of the equilibrium equation to hyper-geometric functions, a new variable is used.

2- Deriving general differential equation

Fig. 1 shows an element of the disk with variable thickness. In this section, only basic equations are needed to be discussed and the way they are obtained is ignored, because in many previous works, these relations have been obtained [27]. Then, the equilibrium equation of rotating disks in displacement variable with arbitrary variable thickness and variable density along the radius also under thermal load can be written as:

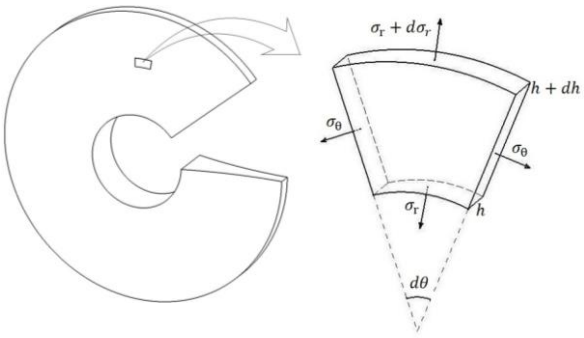

Fig. 1 An element of the disk with variable thickness.

$$\frac{d^2u}{dr^2}+\left(\frac{1}{h}\cdot\frac{dh}{dr}+\frac{1}{r}\right)\cdot\frac{du}{dr}+\left(\frac{\nu}{h\cdot r}\cdot\frac{dh}{dr}-\frac{1}{r^2}\right)\cdot u$$
$$=(1+\nu)\cdot\alpha\cdot\left(\frac{dT}{dr}+\frac{T}{h}\cdot\frac{dh}{dr}\right)-(1-\nu^2)\cdot\frac{\gamma\cdot\omega^2\cdot r}{E} \quad (1)$$

where, u, r, h, γ, T, ω, E, ν and α are radial displacement, radial coordinate, thickness, density, temperature gradient, constant angular velocity, Young modulus, Poisson ratio and linear expansion coefficient of the material, respectively. Of the above coefficients, the coefficients ω, E, ν and α are constant values and other coefficients are functions of coordinate r, The relationship between stresses and radial displacement can be written as follows:

$$\begin{cases}\sigma_r=\dfrac{E}{1-\nu^2}\cdot\left[\left(\dfrac{du}{dr}-\alpha\cdot T\right)+\nu\cdot\left(\dfrac{u}{r}-\alpha\cdot T\right)\right]\\ \sigma_t=\dfrac{E}{1-\nu^2}\cdot\left[\left(\dfrac{u}{r}-\alpha\cdot T\right)+\nu\cdot\left(\dfrac{du}{dr}-\alpha\cdot T\right)\right]\end{cases} \quad (2)$$

where, σ_r and σ_t are the radial and tangential stresses.

In this study, a method called finite element Galerkin method for solving equilibrium Eq. (1) was used and its purpose is to derive an element stiffness matrix that establishes a relation between nodal displacements and external forces. Although a disk is a three-dimensional object, but because of symmetry, it can be avoided in two dimensions as is clear in Eq. (1), displacement and other parameters are only functions of r coordinate. Therefore, the finite element method should be applied to axisymmetric problems. In continuing, Galerkin method [28] is fully expressed in detail.

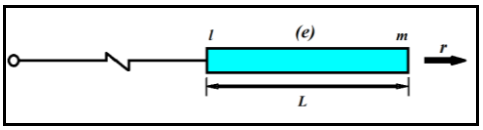

Fig. 2 One-dimensional simple element.

Because of one-dimensional equilibrium Eq. (1), so it should be used a linear approximation. Take Fig. 2, this is the simplest element to approximate a one-dimensional element, where the element's geometry is a straight line and the shape function is linear. If the dependent function is called u and the variable is r, the linear displacement approximation is:

$$u = N_l \cdot u_l + N_m \cdot u_m \tag{3}$$

where, N_l and N_m are shape functions for an element and are equal to:

$$N_l = \frac{r_m - r}{r_m - r_l}$$
$$N_m = \frac{r - r_l}{r_m - r_l} \tag{4}$$

By applying the Galerkin method on Eq. (1), it can be concluded:

$$\int N_s \cdot \begin{bmatrix} \frac{d^2u}{dr^2} + \left(\frac{1}{h}\cdot\frac{dh}{dr} + \frac{1}{r}\right)\cdot\frac{du}{dr} \\ +\left(\frac{\nu}{h\cdot r}\cdot\frac{dh}{dr} - \frac{1}{r^2}\right)\cdot u \\ -(1+\nu)\cdot\alpha\cdot\left(\frac{dT}{dr} + \frac{T}{h}\cdot\frac{dh}{dr}\right) \\ +(1-\nu^2)\cdot\frac{\gamma\cdot\omega^2\cdot r}{E} \end{bmatrix} \cdot dV = 0 \tag{5}$$

where, dV is volume of the isolate element and in polar coordinates is $r \cdot dr \cdot d\theta \cdot dz$. Variable (r) changes between inner radius r_i and outer radius r_e, variable (z) changes from $-\frac{h}{2}$ to $\frac{h}{2}$ and variable (θ) changes from 0 to 2π. Then Eq. (5) can be written as:

$$\int_{r_i}^{r_e}\int_{-h/2}^{h/2}\int_0^{2\pi} N_s \cdot \begin{bmatrix} \frac{d^2u}{dr^2} + \left(\frac{1}{h}\cdot\frac{dh}{dr} + \frac{1}{r}\right)\cdot\frac{du}{dr} \\ +\left(\frac{\nu}{h\cdot r}\cdot\frac{dh}{dr} - \frac{1}{r^2}\right)\cdot u \\ -(1+\nu)\cdot\alpha\cdot\left(\frac{dT}{dr} + \frac{T}{h}\cdot\frac{dh}{dr}\right) \\ +(1-\nu^2)\cdot\frac{\gamma\cdot\omega^2\cdot r}{E} \end{bmatrix} \cdot r\cdot dr\cdot d\theta\cdot dz = 0 \tag{6}$$

Therefore, by integration in the known intervals it yields:

$$\int_{r_i}^{r_e} N_s \cdot \begin{bmatrix} \frac{d^2u}{dr^2} + \left(\frac{1}{h}\cdot\frac{dh}{dr} + \frac{1}{r}\right)\cdot\frac{du}{dr} \\ +\left(\frac{\nu}{h\cdot r}\cdot\frac{dh}{dr} - \frac{1}{r^2}\right)\cdot u \\ -(1+\nu)\cdot\alpha\cdot\left(\frac{dT}{dr} + \frac{T}{h}\cdot\frac{dh}{dr}\right) \\ +(1-\nu^2)\cdot\frac{\gamma\cdot\omega^2\cdot r}{E} \end{bmatrix} \cdot 2\pi\cdot h\cdot r\cdot dr = 0 \tag{7}$$

The terms of Eq. (7) with the second order partial derivatives are subjected to weak formulation and thus by simplifying it results in:

$$\begin{aligned}&-N_s\cdot h\cdot r\cdot\frac{du}{dr}\Big]_{r_i}^{r_e}\\&+\int_{r_i}^{r_e}\left[h\cdot r\cdot\frac{dN_s}{dr}\cdot\frac{du}{dr}+\left(\frac{h}{r}-\nu\cdot\frac{dh}{dr}\right)\cdot N_s\cdot u\right]\cdot dr\\&=\int_{r_i}^{r_e}N_s\cdot\begin{bmatrix}\left(1-\nu^2\right)\cdot\frac{\gamma\cdot\omega^2\cdot r^2\cdot h}{E}\\-\left(1+\nu\right)\cdot\alpha\cdot\left(h\cdot\frac{dT}{dr}+T\cdot\frac{dh}{dr}\right)\cdot r\end{bmatrix}\cdot dr\end{aligned}\tag{8}$$

The first term of left-hand side of Eq. (8) is related to boundary condition and its value must be obtained. According to Eq. (2) the first derivative of radial displacement u can be written in the following form:

$$\begin{cases}\dfrac{du}{dr}=\dfrac{\left(1-\nu^2\right)\cdot\sigma_r}{E}+\alpha\cdot\left(1+\nu\right)\cdot T-\nu\cdot\dfrac{u}{r}\\[2ex]\dfrac{du}{dr}=\dfrac{\left(1-\nu^2\right)\cdot\sigma_t}{E\cdot\nu}+\alpha\cdot\left(\dfrac{1+\nu}{\nu}\right)\cdot T-\dfrac{u}{r\cdot\nu}\end{cases}\tag{9}$$

where the first one is related to σ_r boundary conditions and the other one is for and σ_t boundary conditions. By substituting Eq. (9) into first term of Eq. (8), that means $-N_s\cdot h\cdot r\cdot\frac{du}{dr}\Big]_{r_i}^{r_e}$, then it can be written as the following form:

$$\begin{aligned}&-N_s\cdot h\cdot r\cdot\frac{du}{dr}\Big]_{r_i}^{r_e}=N_s\cdot h\cdot\nu\cdot u\Big]_{r_i}^{r_e}\\&-N_s\cdot h\cdot r\cdot\left[\alpha\cdot\left(1+\nu\right)\cdot T+\frac{\left(1-\nu^2\right)\cdot\sigma_r}{E}\right]_{r_i}^{r_e}\end{aligned}\tag{10}$$

or

$$\begin{aligned}&-N_s\cdot h\cdot r\cdot\frac{du}{dr}\Big]_{r_i}^{r_e}=N_s\cdot h\cdot\frac{u}{\nu}\Big]_{r_i}^{r_e}\\&-N_s\cdot h\cdot r\cdot\left[\alpha\cdot\left(\frac{1+\nu}{\nu}\right)\cdot T+\frac{\left(1-\nu^2\right)\cdot\sigma_t}{E\cdot\nu}\right]_{r_i}^{r_e}\end{aligned}$$

Now, for the master element and node (l) and (m), Eq. (8) converts to the following form:

$$\begin{aligned}&s=l\Rightarrow\int_{r_l}^{r_m}\begin{bmatrix}h\cdot r\cdot\dfrac{dN_l}{dr}\cdot\dfrac{du}{dr}\\+\left(\dfrac{h}{r}-\nu\cdot\dfrac{dh}{dr}\right)\cdot N_l\cdot u\end{bmatrix}\cdot dr\\&=\int_{r_l}^{r_m}N_l\cdot C\cdot dr\\&s=m\Rightarrow\int_{r_l}^{r_m}\begin{bmatrix}h\cdot r\cdot\dfrac{dN_m}{dr}\cdot\dfrac{du}{dr}\\+\left(\dfrac{h}{r}-\nu\cdot\dfrac{dh}{dr}\right)\cdot N_m\cdot u\end{bmatrix}\cdot dr\\&=\int_{r_l}^{r_m}N_m\cdot C\cdot dr\end{aligned}\tag{11}$$

where C is equal to:

$$\begin{aligned}&C=\left(1-\nu^2\right)\cdot\frac{\gamma\cdot\omega^2\cdot r^2\cdot h}{E}\\&-\left(1+\nu\right)\cdot\alpha\cdot\left(h\cdot\frac{dT}{dr}+T\cdot\frac{dh}{dr}\right)\cdot r\end{aligned}\tag{12}$$

It should be noted that in Eq. (11), the term of $-N_s\cdot h\cdot r\cdot\frac{du}{dr}\Big]_{r_i}^{r_e}$ is zero because the amount of N_s at nodes except nodes of master element is zero. Substituting for u its value from Eq. (3) into relations (11) yields:

$$\left\{\int_{r_l}^{r_m}\left[h\cdot r\cdot\frac{dN_l}{dr}\cdot\frac{dN_l}{dr}+\left(\frac{h}{r}-\nu\cdot\frac{dh}{dr}\right)\cdot N_l\cdot N_l\right]\cdot dr\right\}\cdot u_l+$$

$$\left\{\int_{r_l}^{r_m}\left[h\cdot r\cdot\frac{dN_l}{dr}\cdot\frac{dN_m}{dr}+\left(\frac{h}{r}-\nu\cdot\frac{dh}{dr}\right)\cdot N_l\cdot N_m\right]\cdot dr\right\}\cdot u_m=\int_{r_l}^{r_m}N_l\cdot C\cdot dr$$

and

$$\left\{\int_{r_l}^{r_m}\left[h\cdot r\cdot\frac{dN_m}{dr}\cdot\frac{dN_l}{dr}+\left(\frac{h}{r}-\nu\cdot\frac{dh}{dr}\right)\cdot N_m\cdot N_l\right]\cdot dr\right\}\cdot u_l+ \tag{13}$$

$$\left\{\int_{r_l}^{r_m}\left[h\cdot r\cdot\frac{dN_m}{dr}\cdot\frac{dN_m}{dr}+\left(\frac{h}{r}-\nu\cdot\frac{dh}{dr}\right)\cdot N_m\cdot N_m\right]\cdot dr\right\}\cdot u_m=\int_{r_l}^{r_m}N_m\cdot C\cdot dr$$

The purpose of Galerkin method is to derive a relationship between external forces exerted on the nodes and nodal displacements as expressed at the first of this section. This relationship for an element can be expressed by a matrix called the stiffness matrix and, it is a (2×2) matrix for the straight element. Schematically this relationship can be written in the following form:

$$\begin{Bmatrix} f_l \\ f_m \end{Bmatrix}=\begin{bmatrix}\int_{r_l}^{r_m}N_l\cdot C\cdot dr \\ \int_{r_l}^{r_m}N_m\cdot C\cdot dr\end{bmatrix} \tag{14}$$

Thus, according to relation (13) the stiffness matrix of an element can be written in the following form and this is the most important part of this project.

$$\left[K_{lm}^{e}\right]=\begin{bmatrix}\int_{r_l}^{r_m}\left[h\cdot r\cdot\frac{dN_l}{dr}\cdot\frac{dN_l}{dr}+\left(\frac{h}{r}-\nu\cdot\frac{dh}{dr}\right)\cdot N_l\cdot N_l\right]\cdot dr & \int_{r_l}^{r_m}\left[h\cdot r\cdot\frac{dN_l}{dr}\cdot\frac{dN_m}{dr}+\left(\frac{h}{r}-\nu\cdot\frac{dh}{dr}\right)\cdot N_l\cdot N_m\right]\cdot dr \\ \int_{r_l}^{r_m}\left[h\cdot r\cdot\frac{dN_m}{dr}\cdot\frac{dN_l}{dr}+\left(\frac{h}{r}-\nu\cdot\frac{dh}{dr}\right)\cdot N_m\cdot N_l\right]\cdot dr & \int_{r_l}^{r_m}\left[h\cdot r\cdot\frac{dN_m}{dr}\cdot\frac{dN_m}{dr}+\left(\frac{h}{r}-\nu\cdot\frac{dh}{dr}\right)\cdot N_m\cdot N_m\right]\cdot dr\end{bmatrix} \tag{15}$$

and the force matrix $\{F\}$ becomes:

$$\begin{Bmatrix} f_l \\ f_m \end{Bmatrix}=\begin{bmatrix}\int_{r_l}^{r_m}N_l\cdot C\cdot dr \\ \int_{r_l}^{r_m}N_m\cdot C\cdot dr\end{bmatrix} \tag{16}$$

After that, the global stiffness matrix of whole structure can be derived by a reasonable meshing and assembling stiffness matrix of all elements. The common nodes must be assembled. The number of global stiffness matrix arrays is

dependent on the number of nodes. Remember the first term of relation (10) which relates to the boundary conditions was omitted. Now after determining the global stiffness matrix, the removed term can be added to the first and last array of the global stiffness matrix and forces matrix, because they are related to boundary conditions in the first and last nodes. According to relation (14) the amounts of nodal displacements can be derived by multiplying the inverse of global stiffness into the force matrix, so:

$$\{U\}=[K]^{-1}\cdot\{F\} \tag{17}$$

where U is total nodes displacement, K is global stiffness matrix and F is total nodes forces. After that, the amount of radial and tangential stresses can be found from Eq. (2). It should be noted that first it is necessary to find the displacement variation along the elements by using relations (3) and (4). Then by using relation (2) the values of stresses can be derived.

3- Analytical method

At this part, an analytical procedure for non-uniform variable thickness with the following disk profile thickness function is presented.

$$h=h_0\cdot(1-m\cdot r)^k=h_0\cdot(1-x)^k \tag{18}$$

where m, k, h_0 are the geometric specifications and $x=m\cdot r$ is dimensionless variable. By substituting Eq. (18) into Eq. (1) it is concluded that:

$$\begin{aligned}&r\cdot(m\cdot r-1)\cdot\frac{d^2u}{dr^2}+\left[(k+1)\cdot m\cdot r-1\right]\cdot\frac{du}{dr}\\&+\left[(\nu\cdot k-1)\cdot m+\frac{1}{r}\right]\cdot u\\&=(1+\nu)\cdot\alpha\cdot\left[m\cdot\frac{dT}{dr}\cdot r^2-\frac{dT}{dr}\cdot r+m\cdot k\cdot r\cdot T\right]\\&-\frac{(1-\nu^2)\cdot\gamma\cdot\omega^2}{E}\cdot(m\cdot r^3-r^2)\end{aligned} \tag{19}$$

or with respect to variable x:

$$\begin{aligned}&x\cdot(1-x)\cdot\frac{d^2u}{dx^2}+\left[1-(k+1)\cdot x\right]\cdot\frac{du}{dt}\\&+\frac{1}{x}\cdot\left[(1-\nu\cdot k)\cdot x-1\right]\cdot u\\&=\frac{(1-\nu^2)\cdot\omega^2\cdot r_e^3}{E\cdot n^3}\cdot(x^3-x^2)\cdot\gamma\\&+\frac{(1+\nu)\cdot\alpha\cdot r_e}{n}\cdot\left[x\cdot\frac{dT}{dx}-x^2\cdot\frac{dT}{dx}-x\cdot k\cdot T\right]\end{aligned} \tag{20}$$

4- Homogeneous solution

Eq. (20) has a homogeneous solution and two particular solutions due to thermal load and centrifugal load. In order to gain the homogeneous solution of Eq. (20), it defines:

$$\begin{aligned}&x\cdot(1-x)\cdot\frac{d^2u}{dx^2}+\left[1-(k+1)\cdot x\right]\cdot\frac{du}{dx}\\&+\frac{1}{x}\cdot\left[(1-\nu\cdot k)\cdot x-1\right]\cdot u=0\end{aligned} \tag{21}$$

Here, introduces a new variable in form of $u(x)=x\cdot\psi(x)$ and this is the second important part of the project. By substituting first and second derivative of the variable $\psi(x)$ into relation (21) it can be concluded that:

$$\begin{aligned}&x\cdot(1-x)\cdot\frac{d^2\psi}{dx^2}+\left[3-(k+3)\cdot x\right]\cdot\frac{d\psi}{dx}\\&-k\cdot(1+\nu)\cdot\psi=0\end{aligned} \tag{22}$$

This equation is well known as Gauss hyper-geometric differential equation. In general case, hyper-geometric differential

equation [29] is written in the following form:

$$y(z)=A_1\cdot y_1(z)+A_2\cdot y_2(z) \tag{23}$$

where, $y_1(z)$ and $y_2(z)$ becomes:

$$\begin{aligned} y_1(z)&=F(a,b;a+b+1-c;1-z)\\ y_2(z)&=(1-z)^{c-a-b}\\ &\cdot F(c-a,c-b;c-a-b+1;1-z)\end{aligned} \tag{24}$$

In Eq. (25), function F is a hyper-geometric series that defines as [30]:

$$\begin{aligned} F([a,b],c;z)&=\sum_{n=0}^{\infty}\frac{(a)_n\cdot(b)_n}{(c)_n}\cdot\frac{z^n}{n!}\\ &=1+\frac{a\cdot b}{1\cdot c}\cdot z+\frac{a\cdot(a+1)\cdot b\cdot(b+1)}{1\cdot 2\cdot c\cdot(c+1)}\cdot z^2\\ &+\frac{a\cdot(a+1)\cdot(a+2)\cdot b\cdot(b+1)\cdot(b+2)}{1\cdot 2\cdot 3\cdot c\cdot(c+1)\cdot(c+2)}\cdot z^3+\cdots\end{aligned} \tag{25}$$

Nevertheless, the values of a, b and c for Eq. (22) are equal:

$$\begin{cases} a=\dfrac{2+k-\sqrt{k^2-4\cdot k\cdot v+4}}{2}\\ b=\dfrac{2+k+\sqrt{k^2-4\cdot k\cdot v+4}}{2}\\ c=3\end{cases} \tag{26}$$

Therefore, the two linear independent solutions of Eq. (22) can be written in the below form:

$$\begin{aligned} \psi_1(x)&=F(a,b;a+b+1-c;1-x)\\ \psi_2(x)&=(1-x)^{c-a-b}\\ &\cdot F(c-a,c-b;c-a-b+1;1-x)\end{aligned} \tag{27}$$

Subsequently, according to a new variable $u(x)=x\cdot\psi(x)$ that was defined in the previous steps, can write:

$$\begin{aligned} u_1(x)&=x\cdot F(a,b;a+b+1-c;1-x)\\ u_2(x)&=x\cdot(1-x)^{c-a-b}\\ &\cdot F(c-a,c-b;c-a-b+1;1-x)\end{aligned} \tag{28}$$

Finally, the homogenous solution of equilibrium equation of non-linearly variable thickness profile (18) is:

$$u_h(x)=A_1\cdot u_1(x)+A_2\cdot u_2(x) \tag{29}$$

or

$$\begin{aligned} u_h(x)&=A_1\cdot x\cdot F(a,b;a+b+1-c;1-x)\\ &+A_2\cdot x\cdot(1-x)^{c-a-b}\\ &\cdot F(c-a,c-b;c-a-b+1;1-x)\end{aligned} \tag{30}$$

Or in the other hands, with respect to variable m:

$$\begin{aligned} u_h(r)&=A_1\cdot(m\cdot r)\cdot F(a,b;a+b+1-c;1-m\cdot r)\\ &+A_2\cdot(m\cdot r)\cdot(1-m\cdot r)^{c-a-b}\\ &\cdot F(c-a,c-b;c-a-b+1;1-m\cdot r)\end{aligned} \tag{31}$$

where, A_1 and A_2 are new integration constants that can be evaluated from the boundary conditions.

5- Particular solution

To gain the particular solution of Eq. (19), it is best to find the solution in one step (including thermal load, centrifugal load with variable density). Now, we shall to assume the function of thermal and density respect to coordinate r, then:

$$\begin{aligned} T&=T_0+\kappa_1\cdot r+\kappa_2\cdot r^2+\kappa_3\cdot r^3\\ \gamma&=\gamma_0+\gamma_1\cdot\frac{r}{r_e}+\gamma_2\cdot\left(\frac{r}{r_e}\right)^2+\gamma_3\cdot\left(\frac{r}{r_e}\right)^3\end{aligned} \tag{32}$$

By substituting Eq. (33) into Eq. (19), the right-hand side of it, can be written in the following compact form:

$$\chi(r)=\chi_1\cdot r+\chi_2\cdot r^2+\chi_3\cdot r^3+\chi_4\cdot r^4+\chi_5\cdot r^5+\chi_6\cdot r^6 \tag{33}$$

where:

$$\begin{cases}\chi_1=\alpha\cdot(1+\nu)\cdot(m\cdot k\cdot T_0-\kappa_1)\\ \chi_2=\alpha\cdot(1+\nu)\cdot(\kappa_1\cdot m-2\cdot\kappa_2+m\cdot k\cdot\kappa_1)+\dfrac{(1-\nu^2)\cdot\omega^2\cdot\gamma_0}{E}\\ \chi_3=\alpha\cdot(1+\nu)\cdot(2\cdot\kappa_2\cdot m-3\cdot\kappa_3+m\cdot k\cdot\kappa_2)-\dfrac{(1-\nu^2)\cdot\omega^2\cdot\left(\gamma_0\cdot m-\dfrac{\gamma_1}{r_e}\right)}{E}\\ \chi_4=\alpha\cdot(1+\nu)\cdot(3\cdot\kappa_3\cdot m+k\cdot\kappa_3\cdot m)-\dfrac{(1-\nu^2)\cdot\omega^2\cdot\left(\gamma_1\cdot m-\dfrac{\gamma_2}{r_e}\right)}{E\cdot r_e}\\ \chi_5=-\dfrac{(1-\nu^2)\cdot\omega^2\cdot\left(\gamma_2\cdot m-\dfrac{\gamma_3}{r_e}\right)}{E\cdot r_e^{\,2}}\\ \chi_6=-\dfrac{(1-\nu^2)\cdot\omega^2\cdot\gamma_3\cdot m}{E\cdot r_e^{\,3}}\end{cases} \tag{34}$$

By paying attention to Eq. (34), the particular solution can be assumed as

$$u_p(r)=\mu_1\cdot r+\mu_2\cdot r^2+\mu_3\cdot r^3+\mu_4\cdot r^4+\mu_5\cdot r^5+\mu_6\cdot r^6 \tag{35}$$

where μ_1, μ_2, μ_3, μ_4, μ_5 and $\mu_6$are constants; and by substituting this relations, along with its first and second derivatives, in Eq. (19) and by equaling to zero the coefficients of various powers in the variable r, the following relations are obtained:

$$\begin{cases}\mu_6=\dfrac{\chi_6}{35\cdot m+(6+\nu)\cdot k\cdot m}\\ \mu_5=\dfrac{\chi_5+35\cdot\mu_6}{24\cdot m+(5+\nu)\cdot k\cdot m}\\ \mu_4=\dfrac{\chi_4+24\cdot\mu_5}{15\cdot mn+(4+\nu)\cdot k\cdot m}\\ \mu_3=\dfrac{\chi_3+15\cdot\mu_4}{8\cdot m+(3+\nu)\cdot k\cdot m}\\ \mu_2=\dfrac{\chi_2+8\cdot\mu_3}{3\cdot m+(2+\nu)\cdot k\cdot m}\\ \mu_1=\dfrac{\chi_1+3\cdot\mu_2}{(1+\nu)\cdot k\cdot m}\end{cases} \tag{36}$$

6- General solution and corresponding displacement state

The general solution of non-homogeneous differential Eq. (19) as a function of r, is

given by a linear combination of the homogenous solution (30) and the particular integral u_p Eq. (36). Thus, the radial displacement function of the non-linearly variable thickness disk can be derived in the following form:

$$u = u_h + u_p \tag{37}$$

By substituting this relation, along with its first derivative in Eq. (2) and at the same time, applying the boundary condition, the integration constants as A_1 and A_2can be found. Moreover, it is possible to express the radial and tangential stresses versus coordinate r.

7- Case studies

Here, we provide some case studies that show the use of the present numerical and analytical formulation outlined. Results determined as per the numerical solution are compared with those obtained by the exact analytical solution in the following figure for all cases. In addition, results for stress function and radial displacement of the rotating variable-thickness annular disks with inner radius ($r_i = 0.1m$) and outer radius ($r_e = 0.8m$) in the following figure are presented. Also, the geometry of the rotors involves a parabolic profile web explained in Eq. (26) and their profiles in each figure have been shown. The material is used in the cases is Inconel-718 has the following specifications: $E = 205Gpa$, $v = 0.284$, $\gamma_0 = 8190\,\frac{kg}{m^3}$, $\alpha = 11.568 \times 10^{-6}$.

In the all cases, the disks are subjected to thermal load and they have variable density along the radius that has been expressed in relations (32) together their distribution curves have been shown in Fig. 3 and Fig. 4.

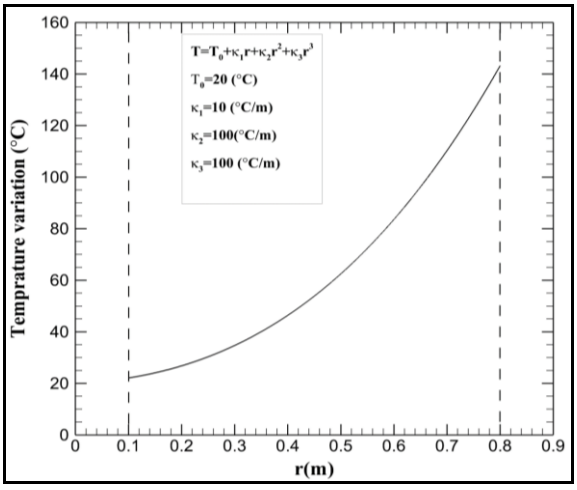

Fig. 3 Temperature variation along the radius

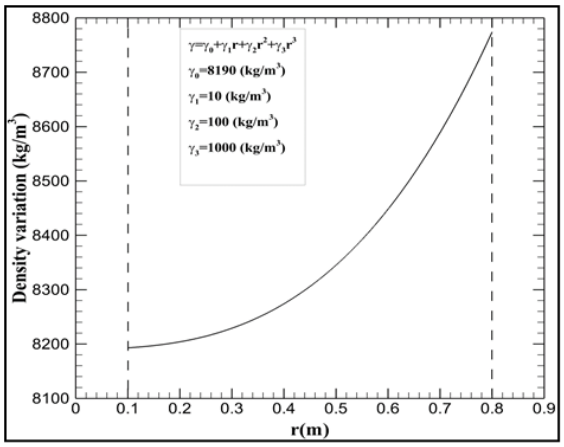

Fig. 4 Density variation along the radius

It should be noted that the angular velocity of all disks is constant and equal to $\omega = 514(rad/s)$.

Here, five different cases were studied, the first three cases without rim and hub and two end discs have been checked with hub and rim.

7-1- Case 1

Fig. 5 and Fig. 6, show displacement distribution and radial and hoop stresses distribution curves as function of r and having temperature gradient and density variation according to Fig. 3 and Fig. 4 for an Inconel-718 annular disk according Eq.

(18) with $(k = 3.5, m = 0.4375)$. It is a concave and convergent profile.

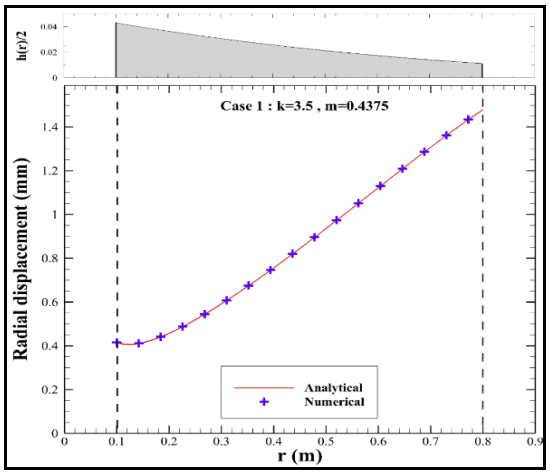

Fig. 5 Numerical and analytical displacement-distribution curve u for case 1

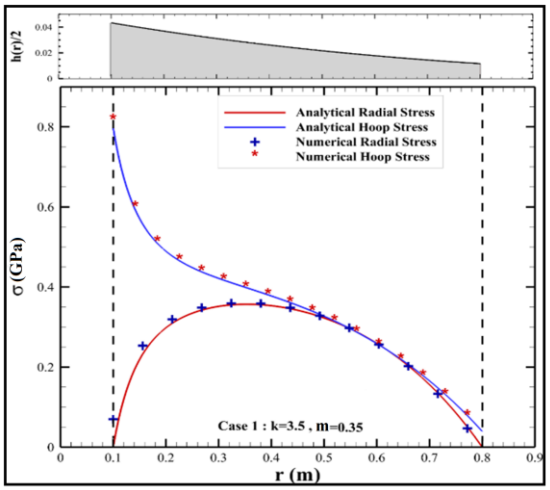

Fig. 6 Numerical and analytical stress-distribution curves σ_r and σ_t for case 1

7-2- Case 2

Figs. 7 and 8, show displacement distribution and radial and hoop stresses distribution curves as function of r and having temperature gradient and density variation according to Figs. 3 and 4 for an Inconel-718 annular disk according Eq. (18) with $(k = 0.5,\ m = 1.1625)$. It is a convex and convergent profile.

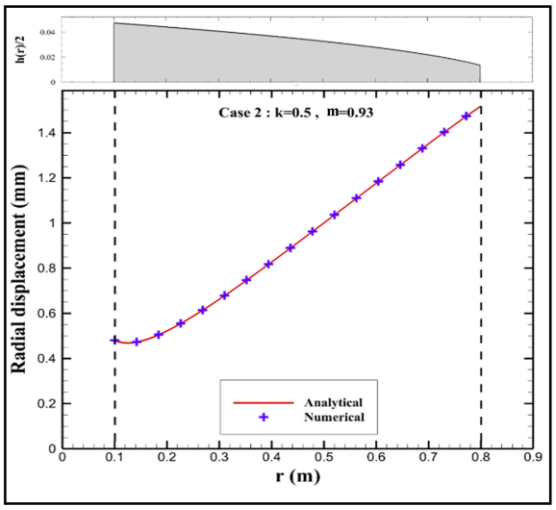

Fig. 7 Numerical and analytical displacement-distribution curve u for case 2

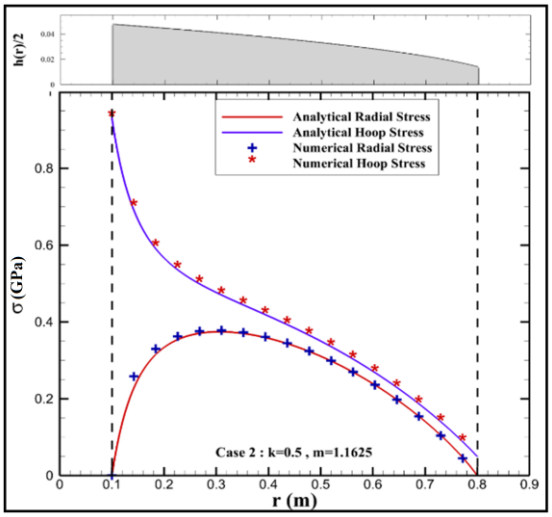

Fig. 8 Numerical and analytical stress-distribution curves σ_r and σ_t for case 2

7-3- Case 3

Fig. 9 and Fig. 10, show displacement distribution and radial and hoop stresses distribution curves as function of r and having temperature gradient and density variation according to Fig. 3 and Fig. 4 for an Inconel-718 annular disk according Eq. (18) with $(k = -3.5, m = 0.4375)$. It is a concave and divergent profile.

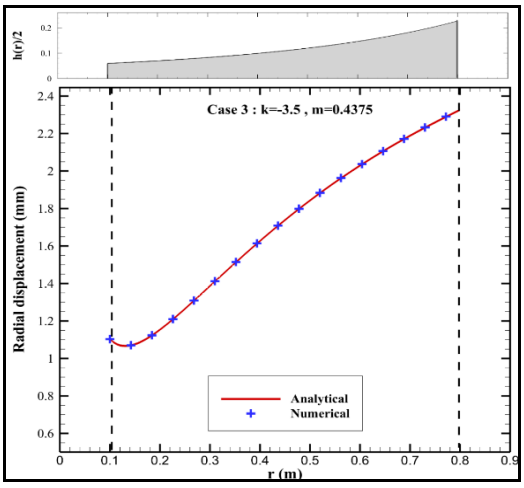

Fig. 9 Numerical and analytical displacement-distribution curve u for case 3

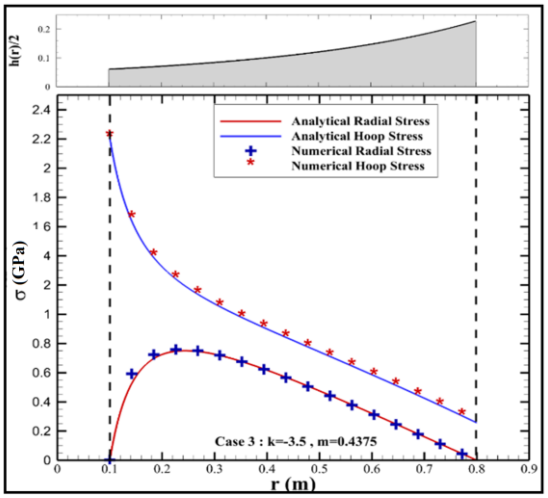

Fig. 10 FEM and analytical stress-distribution curves σ_r and σ_t for case 3

7-4-Case 4

If, as it often happens in turbine and compressor discs, the discs feature a rim and a hub, both of which are considered of constant thickness, it is necessary to determine first of all radial stresses σ_{r_A} and σ_{r_B} which are present in section A ($r = r_i$) and in section B ($r = r_e$), respectively, and which constitute two unknown hyperstatic values. In this practical case, the rim ring is simulated by an axisymmetric radial stress at the outer interface. Fig. 11, Fig. 12 and Fig. 13, show displacement distribution and radial and hoop stresses distribution curves as function of r and having temperature gradient and density variation according to Fig. 3 and Fig. 4 for an Inconel-718 annular disk according Eq. (18) ($k = 3.5, m = 0.4375$) with rim and hub. It is a concave and convergent profile.

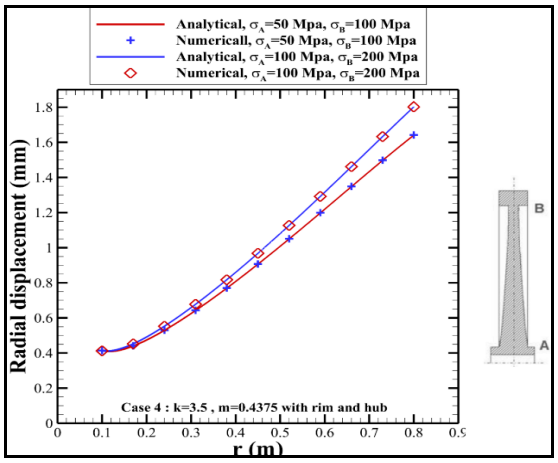

Fig. 11 Numerical and analytical displacement-distribution curve u for case 4

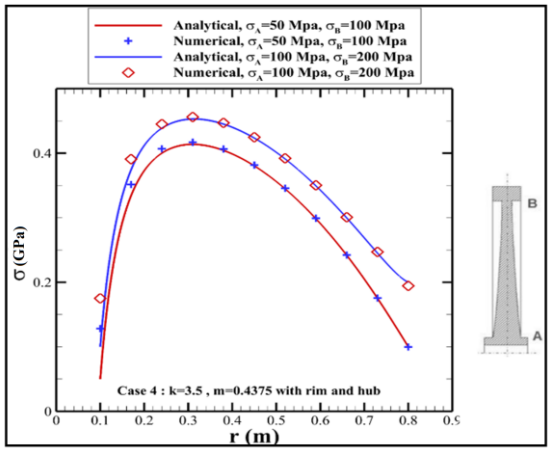

Fig. 12 Numerical and analytical radial stress-distribution curves σ_r for case 4

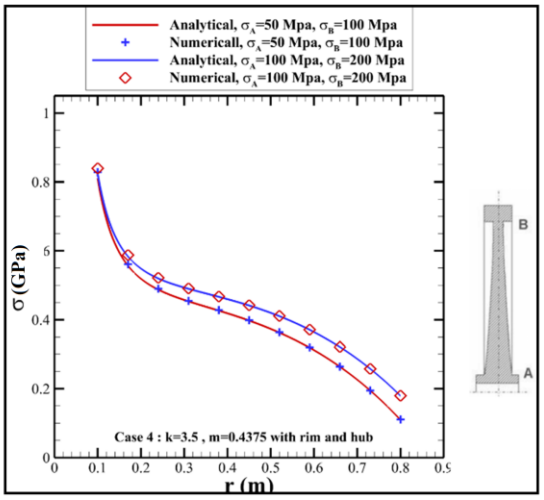

Fig. 13 Numerical and analytical hoop stress-distribution curves σ_t for case 4

7-5- Case 5

Fig. 14, Fig. 15 and Fig. 16, show displacement distribution and radial and hoop stresses distribution curves as function of r and having temperature gradient and density variation according to Fig. 3 and Fig. 4 for an Inconel-718 annular disk according Eq. (18) (k=0.5, m=1.1625) with rim and hub. It is a convex and convergent profile.

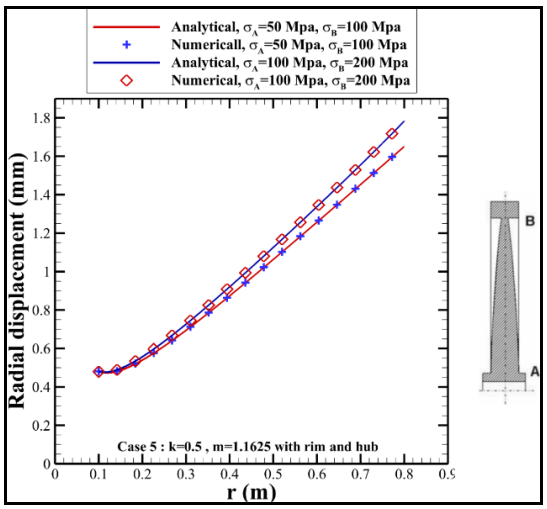

Fig. 14 Numerical and analytical displacement-distribution curve u for case 5

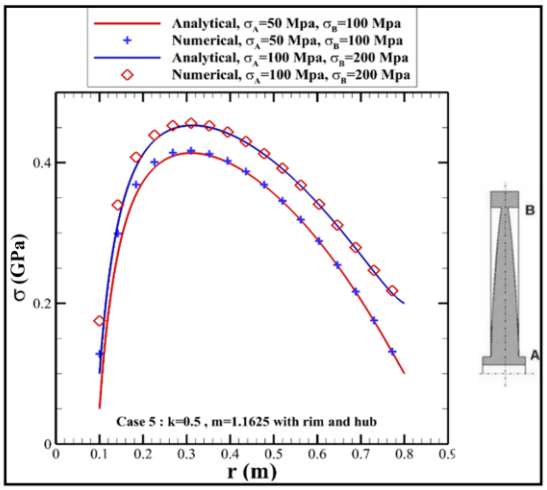

Fig. 15 FEM and analytical radial stress-distribution curves σ_r and σ_t for case 5

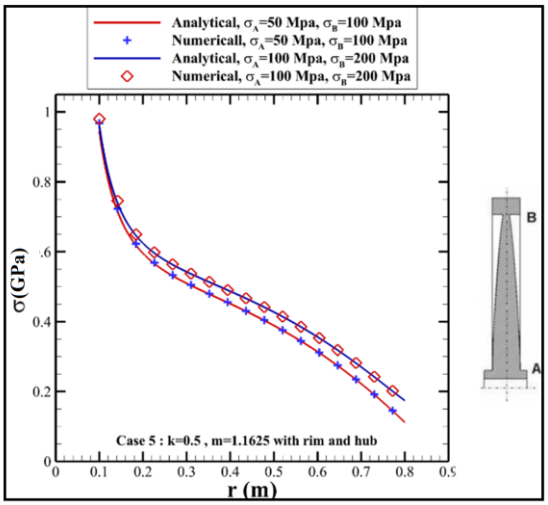

Fig. 16 FEM and analytical hoop stress-distribution curves σ_r and σ_t for case 5

8- Conclusion

In this study, radial displacement and radial and tangential stresses for each type of desired thickness function of symmetrical disk that rotates at a constant rotational speed and under centrifugal load and temperature gradient which has varying density along the radius is obtained. To do this, Galerkin method which is a numerical method was used. It was concluded that the Galerkin method is quite comprehensive, practical and there are not any restrictions to it. In fact, a stiffness matrix element was obtained schematically by selecting the appropriate

number of elements, the matrix values for each rotating disk with arbitrary loading conditions can be acquired and finally nodal displacements can be reckoned. Displacement and stress distribution of some nonlinearly rotating disks with varying densities and under the influence of the temperature gradient along with the hub and rim were obtained using analytical methods, and the results were completely consistent with the results of numerical methods. Thus, it can be concluded that the numerical methods are accurate. Another result of the project, is that using a new variable is that it converts the homogenous part of equilibrium equation to a hyper-geometric differential equation and it makes it extremely easy to solve.

References

[1] Timoshenko, S. (1956). *Strength of Materials: Part 2, Advanced Theory and Problems*. van Nostrand.

[2] Grammel, R. (1936). Neue Lösungen des Problems der rotierenden Scheibe. Ingenieur-Archiv, 7(3), 137-139.

[3] Thompson, A. S. (1946). Stresses in rotating disks at high temperatures.

[4] Pirmoradian, M. (2015). Dynamic stability analysis of a beam excited by a sequence of moving mass particles. Journal of Simulation and Analysis of Novel Technologies in Mechanical Engineering, 8(1), 41-49.

[5] Torkan, E., Pirmoradian, M., & Hashemian, M. (2017). Occurrence of parametric resonance in vibrations of rectangular plates resting on elastic foundation under passage of continuous series of moving masses. Modares Mechanical Engineering, 17(9), 225-236.

[6] Sterner, S. C., Saigal, S., Kistler, W., & Dietrich, D. E. (1994). A unified numerical approach for the analysis of rotating disks including turbine rotors. International journal of solids and structures, 31(2), 269-277.

[7] You, L., Tang, Y., Zhang, J., & Zheng, C. (2000). Numerical analysis of elastic–plastic rotating disks with arbitrary variable thickness and density, International Journal of Solids and Structures, 37(52), 7809-7820.

[8] Torkan, E., & Pirmoradian, M. (2019). Efficient higher-order shear deformation theories for instability analysis of plates carrying a mass moving on an elliptical path. Journal of Solid Mechanics, 11(4), 790-808.

[9] Biezeno, C. B., & Grammel, R. (2013). Technische dynamic. Springer-Verlag.

[10] Dubbel, H. (2013). DUBBEL: Taschenbuch für den Maschinenbau. Springer-Verlag.

[11] Stodola, A. (1924). Mit einem Anhang über die Aussichten der Wärmekraftmaschinen. Springer Berlin.

[12] Honegger, V. E. (1927). Festigkeitsberechnung von rotierenden konischen Scheiben. ZAMM-Journal of Applied Mathematics and Mechanics/Zeitschrift für Angewandte Mathematik und Mechanik, 7(2), 120-128.

[13] Giovannozzi, R. (1956). Calculation, tabulation and uses of some functions occurring in the theory of the conical disc subjected to centrifugal and thermic stress. Proceedings of II Congresso Aeronautico Europeo (pp. 30.31-30.12), Scheveningen.

[14] Güven, U. (1995). Tresca's yield condition and the linear hardening rotating solid disk of variable thickness. ZAMM-Journal of Applied Mathematics and Mechanics/Zeitschrift für Angewandte Mathematik und Mechanik, 75(10), 805-807.

[15] Orcan, Y., & Eraslan, A. N. (2002). Elastic–plastic stresses in linearly hardening rotating solid disks of variable thickness. Mechanics Research Communications, 29(4), 269-281.

[16] Eraslan, A. N., & Argeso, H. (2002). Limit angular velocities of variable thickness rotating disks. International Journal of Solids and Structures, 39(12), 3109-3130.

[17] Eraslan, A.N. (2005). A class of nonisothermal variable thickness rotating disk problems solved by hypergeometric functions. Turkish Journal of Engineering and Environmental Sciences, 29(4), 241-269.

[18] Vivio, F., & Vullo, V. (2007). Elastic stress analysis of rotating converging conical disks subjected to thermal load and having variable

density along the radius. *International Journal of Solids and Structures*, 44(24), 7767-7784.

[19] Hojjati, M., & Jafari, S. (2008). Semi-exact solution of elastic non-uniform thickness and density rotating disks by homotopy perturbation and Adomian's decomposition methods. Part I: Elastic solution. International Journal of Pressure Vessels and Piping, 85(12), 871-878.

[20] Zenkour, A. M., & Mashat, D. S. (2010). Analytical and numerical solutions for a rotating annular disk of variable thickness. Applied Mathematics, 1(5), 431.

[21] Zenkour, A. M., & Mashat, D. S. (2011). Stress function of a rotating variable-thickness annular disk using exact and numerical methods. Engineering, 3(4), 422.

[22] Nejad, M. Z., Jabbari, M., & Ghannad, M. (2014). A semi-analytical solution for elastic analysis of rotating thick cylindrical shells with variable thickness using disk form multilayers. The Scientiic World Journal, Vol. 2014, ID 932743, 10 pages.

[23] Zamani Nejad, M., Jabbari, M., & Ghannad, M. (2014). Elastic Analysis of Rotating Thick Truncated Conical Shells Subjected to Uniform Pressure Using Disk Form Multilayers. ISRN Mechanical Engineering, Vol. 2014, http://dx.doi.org/10.1155/2014/764837

[24] Bagheri, E., Asghari, M., & Danesh, V. (2019). Analytical study of micro-rotating disks with angular acceleration on the basis of the strain gradient elasticity. Acta Mechanica, 230(9), 3259-78.

[25] Abdalla, H.M., Casagrande, D., & Moro, L. (2020). Thermo-mechanical analysis and optimization of functionally graded rotating disks. The Journal of Strain Analysis for Engineering Design, 55(5-6), 159-71.

[26] Sharma, D., Kaur, R., & Sharma, H. (2021). Investigation of thermo-elastic characteristics in functionally graded rotating disk using finite element method. Nonlinear Engineering, 10(1), 312-22.

[27] Vullo, V., & Vivio, F. (2013). Rotors: Stress analysis and design, Springer Science & Business Media.

[28] Zienkiewicz, O. C., Taylor, R. L., & Zhu, J. Z. (2005). The finite element method: its basis and fundamentals. Elsevier.

[29] Gasper, G., Rahman, M., & George, G. (2004). Basic hypergeometric series. Cambridge university press.

[30] Aomoto, K., Kita, M., Kohno, T., & Iohara, K. (2011). Theory of hypergeometric functions. Springer.